Can we water crops with our phones? Smartphone technology application to infrared thermography for use in irrigation management

J. Puértolas*, D. Johnson, I.C. Dodd and S.A. Rothwell,
Lancaster Environment Centre, Lancaster University, United Kingdom

Abstract

Infrared thermography has been used to assess plant transpiration and infer stress levels in different agricultural production systems. The development of low cost infrared cameras adapted to smart phones provides an opportunity to develop applications that would allow growers to monitor crop water status. We explored the capabilities of this system by assessing the response of crop water stress index (CWSI) to treatments differing in irrigation frequency. Soya bean plants were grown in pots in a glasshouse and different irrigation treatments were applied for two weeks. CWSI, stomatal conductance (g_s) and biomass growth were compared in fully irrigated (FI), deficit irrigation (50% ET) applied either at high (HFDI) and low (LFDI) frequency. Statistical differences in CWSI between deficit irrigation and FI treatments were observed when CWSI>0.5. CWSI and g_s followed very similar patterns in all treatments, but the higher number of replicates that the thermal camera could measure in a given time and its low variability compared to the porometer increased the capacity to detect differences between treatments. As g_s decreased at the end of the experiment in FI plants, probably because of restricted soil volume, differences in CWSI between well-watered and stressed plants diminished, suggesting the need to maintain well-watered plants grown under optimal conditions as a reference baseline. Within the deficit irrigation treatments, CWSI decreased and g_s, increased when irrigation was more frequent, but dry biomass and water use efficiency (biomass / irrigation volume) did not change, and were lower and higher than FI plants respectively. These results demonstrate that the low cost thermal camera is suitable to rapidly assess g_s, but highlight the issues associated with irrigation scheduling based on this physiological response.

Keywords: stomatal conductance, deficit irrigation, *Glycine max*, irrigation frequency, crop water stress index

INTRODUCTION

The application of precision irrigation techniques that maximise water use efficiency currently rely on developing tools that accurately measure the availability of resources to the crop. The most precise way to monitor the effect of water availability on crop performance is to use plant-based sensors (Jones, 2004). Different tools to monitor plant physiological status have been previously used in precision irrigation (Fernández, 2014), but they generally require relatively high investment and a certain degree of training in plant physiology. Smartphone technology is an affordable and easy-to-use option to monitor plant water status and schedule irrigation. Among the numerous gadgets that can be attached to or integrated within smartphones, small thermal cameras are the most promising (Skewes et al., 2018).

The cooling effect of transpiration is the basis of using thermal imaging to estimate plant transpiration and detect water stress (Maes and Steppe, 2012). This method has received considerable attention over the last decades and farmers use it now as a precision irrigation tool. Applying smartphone-based thermal imaging may be beneficial in large

commercial farms, as it would reduce considerably the costs, but also has potential for use by smallholder farmers in developing countries, as phones are now widely and affordably available in any part of the world. However, developing this technology for irrigation scheduling requires research on the capability of these devices to assess plant transpiration, and predict water stress.

Deficit irrigation scheduling relies on a good understanding of crop physiological responses to drought. Reducing irrigation volume modifies the spatial and temporal distribution of soil water, which result in different responses depending on the frequency of the irrigation (Boyle et al., 2016). Smartphone-based thermal imaging could be an easy and fast method to determine plant response to these complex changes of soil moisture by estimating the stomatal closure. However, since stomatal responses can be altered by pronounced soil moisture gradients generated during deficit irrigation, the relation between stomatal conductance and plant growth needs to be assessed.

This study aimed to determine the suitability of smartphone-based thermal imaging to estimate stomatal conductance and schedule deficit irrigation. Potted soya bean plants were subjected to different deficit irrigation treatments with varying frequency of application, and stomatal conductance estimated by thermal imaging and porometry. We hypothesised that i) Temperature measurements from smartphone-adapted thermal cameras are accurate enough to predict stomatal conductance, ii) these predictions can determine the degree of plant water stress to assist in deficit irrigation scheduling.

MATERIAL AND METHODS

Soya bean (*Glycine max* 'Siverka') seeds were sown in sixty 3 L pots containing an organic loamy compost (John Innes N2, Westland, UK) and grown for four weeks in an unheated greenhouse (maximum temperature 26°C, minimum 16°C). During the photoperiod (14 hours), when natural light was below 200 µmol m^{-2} s^{-1}, light was supplied by lamps providing 400 µmol m^{-2} s^{-1}. Plants were irrigated daily and fertigated weekly with a commercial soluble fertiliser (All Purpose, MiracleGro, USA). At the end of the third week, twelve plants were assigned randomly to each of 3 irrigation treatments:

FI: Full irrigation; 100% of evapotranspiration replaced daily at 12:00. HFDI: High frequency deficit irrigation; 50% of FI water applied daily. LFDI: Low frequency deficit irrigation; water withheld in cycles of four days and 50% of accumulated FI water during the cycle applied.

Stomatal conductance and leaf temperature were measured in one fully expanded sunlit leaf per plant. Before applying the treatments, leaves were selected and marked to facilitate their identification in the thermal picture by attaching a letter-shaped piece of paper. In the middle of the experiment, the mark was shifted to an upper leaf to avoid ageing and self-shading effects on g_s. Photographs were taken daily within 10 minutes, three hours before irrigation and immediately before porometry measurements. Six pictures were needed to capture the 36 plants of the experiment. For each picture, two 100 cm^2 grey cardboard references (wet and dry) were used to calculate CWSI values. Overhead photographs of the canopy were taken with a thermal camera (FLIR One, FLIR, UK) attached to a smartphone (Galaxy S6, Samsung, UK) from 1 m above the canopy and analysed with FLIR Tools software (FLIR, UK). The temperature of the marked leaf (T_{leaf}) in each plant and references (T_{dry}, T_{wet}) was averaged from 2-3 points and CWSI calculated as $CWSI=(T_{leaf} - T_{wet})/(T_{dry}-T_{wet})$. CWSI was selected as the preferred index since it can be easily calculated from thermal imaging (Maes and Steppe, 2012). Stomatal conductance was measured in two of the three leaflets of the marked leaf with a porometer (AP4, Delta-T Devices, UK) in a subsample of 6 plants per treatment. Porometry measurements took 30-35 minutes.

After two weeks of applying treatments, all plants were harvested to determine shoot and root dry weight and retrospectively calculate substrate gravimetric water content based on actual substrate dry weight, and the pot weight measured before each irrigation (plant weight was considered negligible as it was <2% of the total soil weight). The substrate was

dried in an oven at 70°C for one week until constant mass. Applied water use efficiency (WUE) was calculated for each treatment by dividing plant biomass by the total volume of irrigation.

Statistical analyses

Statistical differences for all the variables were analysed by simple ANOVA. Statistical differences among treatments were assessed with the Tukey post-hoc test with SPSS 24 (IBM, USA). Relationships between CWSI and g_s were assessed by nonlinear regression and fitted to a hyperbolic decay curve with SigmaPlot (Systat Software, USA).

RESULTS

Soil gravimetric water content (θ_g) in FI was always above 0.9 g g^{-1} (Fig. 1a), which according to a soil moisture release curve corresponded to soil matric potentials above -10 kPa (data not shown). The LFDI treatment rapidly decreased θ_g to 0.4 g g^{-1} (-125 kPa) within 4 days, which increased after re-watering. θ_g after re-watering declined progressively, but it was relatively high after the last irrigation on day 12,(0.7 g g^{-1}; -40 kPa). θ_g in The HFDI treatment rapidly decreased θ_g during the first week down to 0.5 g g^{-1} (-100 kPa) and more slowly on the following week..

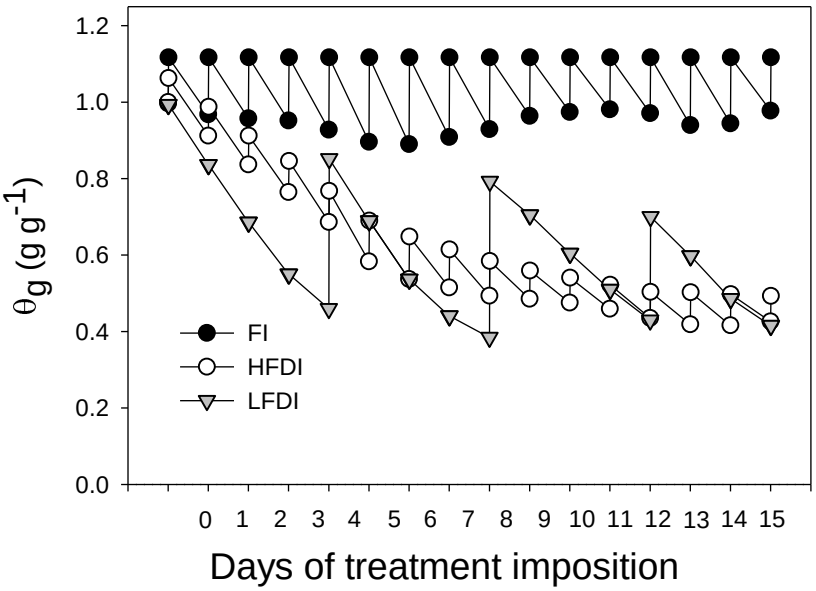

Figure 1. Soil gravimetric water content (θ_g) (n=12) during the application of treatments. FI: Full irrigation (depicted in both panels for comparison, black circles); HFDI: High frequency irrigation (white circles); LFDI: Low frequency irrigation treatments (gray inverted triangles). Standard errors smaller than the symbols and not depicted.

Stomatal conductance decreased after withholding water in LFDI and recovered the day after re-watering (Fig. 2a). HFDI and FI showed a less distinctive pattern, but HFDI was generally lower than FI and higher than LFDI except after re-watering of the latter. However, due to high variability, there were no statistical differences between HFDI and LFDI (except on day 4, at the end of the first LFDI cycle) or FI (except for the last four days of the experiment). After the second cycle of LFDI (~10 days after imposing treatments), g_s declined steadily in all the treatments including FI.

CWSI followed a similar pattern to g_s, but the statistical significance in the difference between treatments was higher, probably because of lower standard errors (Fig 2b), which

were caused by both larger sample size and lower variability. For instance, on day 7, the coefficient of variation (C.V.) of g_s in the different treatments was 63, 55, and 70% for FI, HFDI and LFDI respectively, while it was 7, 32 and 20% for CWSI in the same plants where g_s was measured. Hence, CWSI values in FI were more stable than g_s (around 0.3) and increased steadily over the last 4 days of the experiment.

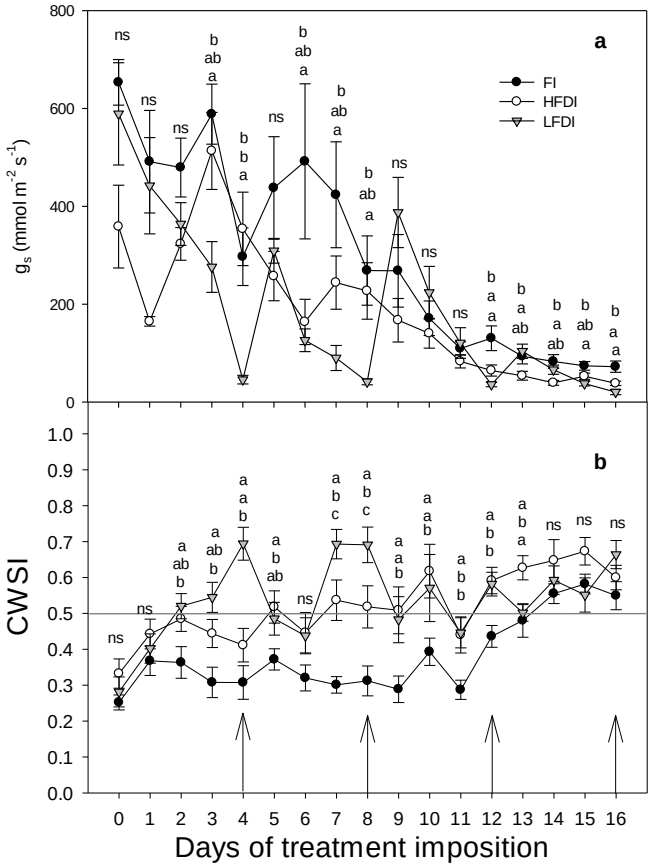

Figure 2. Stomatal conductance (g_s) (a) and Crop Water Stress Index (CWSI) (b) during treatment application (mean±s.e.; n=12). FI: Full irrigation (black circles); HFDI: High frequency irrigation (white circles); LFDI: Low frequency irrigation treatments (gray inverted triangles). In panel b, arrows indicate irrigation day for LFDI. The horizontal line mark the CWSI=0.5 threshold for reference. Different letters denote differences between treatments (FI: upper letter, HFDI: middle, LFDI: lower).

CWSI and g_s were correlated but the relationship was not strong (Fig. 3), as plants with lower g_s sometimes had low CWSI values. However, leaves with high g_s (>200 mmol $m^{-2}s^{-1}$) had always CWSI<0.5.

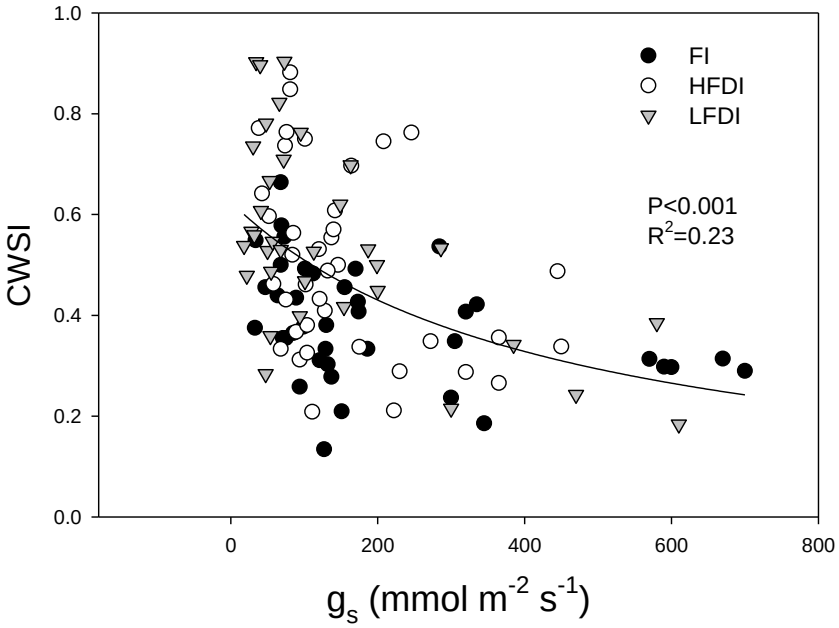

Figure 3. Relationship between Crop Water Stress Index (CWSI) and stomatal conductance (g_s) in individual leaves. FI: Full irrigation (depicted in both panels for comparison, black circles); HFDI: High frequency irrigation (white circles); LFDI: Low frequency irrigation treatments (gray inverted triangles). Nonlinear regression curve (hyperbolic decay), P-value and R^2 for the pooled dataset are depicted.

Dry biomass was higher in FI than the two deficit irrigation treatments, which did not differ (Table 1). WUE followed the inverse pattern, with higher WUE in the deficit irrigation treatments than in FI**.**

Table 1., Shoot and root dry weight (DW) and water use efficiency (WUE) for the three irrigation treatments (FI: Full irrigation; HFDI: High frequency deficit irrigation; LFDI: Low frequency deficit irrigation). Mean±s.e, n=12. Different letters denote statistical differences between treatments (Tukey, P<0.05)

Treatment	**Shoot DW (g)**	**Root DW (g)**	**$WUE_{applied}$ (g l^{-1})**
FI	8.52±0.23 b	1.13±0.04 b	4.87±0.19 a
HFDI	6.51±0.25 a	0.83±0.03 a	7.22±0.27 b
LFDI	6.11±0.20 a	0.82±0.04 a	7.40±0.38 b

DISCUSSION

The good agreement between g_s and CWSI evolution during the experiment (Fig. 2) confirmed that this thermal camera was sufficiently accurate to capture differences in physiological status across treatments, as in woody crops such grapevine and almond which were compared against high-end thermal cameras (around 20-fold more expensive) with satisfactory results (Skewes et al., 2018; García-Tejero et al., 2018). Average CWSI values above 0.5 in deficit irrigation treatments were generally statistically different from FI, which typically was 0.3. That value separating stressed from well-watered plants (0.5) could be used as a decision threshold in deficit irrigation scheduling.

The lower variability of CWSI compared to g_s might be because it is a non-invasive technique. This together with the ability to obtain more rapidly an extensive representation of the canopy suggests an overall superior precision to porometry as a tool to detect the physiological status of the different irrigation treatments. However, the correlation between

leaf temperature and stomatal conductance on an individual plant basis was not strong because of the poor relationship at low g_s (Fig. 3). This could be due to the effect of transient shading at the time the picture was taken by the structural beams of the greenhouse roof, which decreased leaf temperature compared to the reference. However, the consistent high g_s of leaves with CWSI<0.5 explains the ability of average values of CWSI to discriminate between deficit and full irrigation treatments.

The decline of g_s over time could be attributed to the effect of root binding as the plant grew in a restricted soil volume (Sinclair et al., 2017). The increase CWSI in FI might make it difficult to use a constant value of this parameter as a threshold for deficit irrigation scheduling. These difficulties are not attributable to limitations of the thermal imaging technique, but in general of the use of g_s as a water stress indicator. Nevertheless, average values of CWSI and g_s still significantly differed between fully irrigated and deficit irrigation treatments (Fig. 2b), suggesting that CWSI thresholds need to be re-evaluated at different stages of the crop by comparing stressed vs. non-stressed plants, so the maintenance of a few irrigated plants as a reference might be necessary (Agam et al., 2013).

Previous studies showed that increased deficit irrigation frequency improved plant g_s at the same overall pot water content, as it creates wetter layers in the upper part of the pot (Puértolas et al., 2017). This explains the intermediate CWSI in HFDI compared to LFDI and FI on many dates during the experiment, in particular at the end of LFDI drying cycles, when overall pot soil moisture was comparable in HFDI and LFDI (Fig. 1, 2a). However, dry matter accumulation and applied water use efficiency depended exclusively on the irrigation volume and not on the frequency of application. This suggests g_s and plant growth are de-coupled, due to the higher sensitivity of plant growth to declining plant water status, implying that carbon demand (growth) is more reduced at higher plant water potential than supply (photosynthesis) (Muller et al., 2011). This highlights a potential limitation of using thermal imaging to improve water use efficiency by efficient deficit irrigation scheduling, as growth limitation is likely to occur before changes in stomatal conductance. More research is needed to determine the variations of carbon assimilation and growth upon re-watering events to assess the extent of this limitation.

ACKNOWLEDGEMENTS

This research was funded by the N8 AgriFood Program through its Local Pump Priming Scheme.

Literature cited

Agam, N., Cohen, Y., Alchanatis, V., and Ben-Gal, A. (2013). How sensitive is the CWSI to changes in solar radiation? International Journal of Remote Sensing *34 (17),* 6109-6120. https://doi.org/10.1080/01431161.2013.793873.

Boyle, R.K.A., McAinsh, M., and Dodd, I.C. (2016). Daily irrigation attenuates xylem abscisic acid concentration and increases leaf water potential of *Pelargonium x hortorum* compared to infrequent irrigation. Physiol. Plant. *158 (1)*, 23-33 https://doi.org/10.1111/ppl.12433.

Fernández, J.E. (2014). Plant-based sensing to monitor water stress: applicability to commercial orchards. Agric. Water Manag. *142*, 99-109 https://doi.org/10.1016/j.agwat.2014.04.017.

García-Tejero, I., Ortega-Arevalo, C.J., Iglesias-Contreras, M., Moreno, J.M., Souza, L., Cuadros Tavira, S., and Durán-Zuazo, V.H. (2018). Assessing the crop-water status in almond (*Prunus dulcis* Mill.) trees via thermal imaging camera connected to smartphone. Sensors *18 (4)*, 1050 https://doi.org/10.3390/s18041050.

Jones, H.G. (2004). Application of thermal imaging and infrared sensing in plant physiology and ecophysiology. Adv. Bot. Res. *41*, 107-163 https://doi.org/10.1016/S0065-2296(04)41003-9.

Maes, W.H., and Steppe, K. (2012). Estimating evapotranspiration and drought stress with ground-based thermal remote sensing in agriculture: a review. J. Exp. Bot. *13 (1)*, 4671-4712 https://doi.org/10.1093/jxb/ers165.

Muller, B., Pantin, F., Génard, M., Turc, O., Freixes, S., Piques, M., and Gibon, Y. (2011). Water deficits uncouple growth from photosynthesis, increase C content, and modify the relationship between C and growth in sink organs, J. Exp. Bot. *62 (6)*, 1715-1729.

Puértolas, J., Larsen, E.K., Davies, W.J., Dodd, I.C. (2017). Applying 'drought' to potted plants by maintaining suboptimal soil moisture improves plant water relations. J. Exp. Bot. *68 (9)*, 2413-2424 https://doi.org/10.1093/jxb/erx116.

Sinclair, T.R., Manandhar, A., Shekoofa, A., Rosas-Anderson, P., Bagherzadi, L., Schoppach, Sadok, W., and Rufty, T.W. (2017). Pot binding as a variable confounding plant phenotype: theoretical derivation and experimental observations. Planta *245 (4)* 729-735 https://doi.org/10.1007/s0042.

Skewes, M., Petrie, P.R., Liu, S., and Whitty, M. (2018). Smartphone tools for measuring vine water status. Acta Hortic. *1197*, 53-58 https://doi.org/10.17660/ActaHortic.2018.1197.